THE JOURNAL OF PHYSICAL CHEMISTRY Letters

Letter

pubs.acs.org/JPCL

Surface Polarization Model for the Dynamic Hysteresis of Perovskite Solar Cells

Sandheep Ravishankar,[†] Osbel Almora,[†] Carlos Echeverría-Arrondo,[†] Elnaz Ghahremanirad,[†,‡] Clara Aranda,[†] Antonio Guerrero,[†] Francisco Fabregat-Santiago,[†] Arie Zaban,[§] Germà Garcia-Belmonte,[†] and Juan Bisquert*[,†]

[†]Institute of Advanced Materials (INAM), Universitat Jaume I, 12006 Castelló, Spain

[‡]Nano-photonics and Optoelectronics Research Laboratory (NORLab), Shahid Rajaee Teacher Training University, 16788-15811 Lavizan, Tehran, Iran

[§]Department of Chemistry, Institute for Nanotechnology & Advanced Materials, Bar-Ilan University, Ramat Gan 52900, Israel

Supporting Information

ABSTRACT: The dynamic hysteresis of perovskite solar cells consists of the occurrence of significant deviations of the current density−voltage curve shapes depending on the specific conditions of measurement such as starting voltage, waiting time, scan rate, and other factors. Dynamic hysteresis is a serious impediment to stabilized and reliable measurement and operation of the perovskite solar cells. In this Letter, we formulate a model for the dynamic hysteresis based on the idea that the cell accumulates a huge quantity of surface electronic charge at forward bias that is released on voltage sweeping, causing extra current over the normal response. The charge shows a retarded dynamics due to the slow relaxation of the accompanying ionic charge, that produces variable shapes depending on scan rate or poling value and time. We show that the quantitative model provides a consistent description of experimental results and allows us to determine significant parameters of the perovskite solar cell for both the transient and steady-state performance.

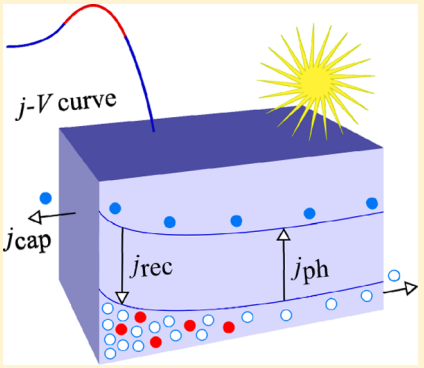

Lead halide perovskite has established a major scientific and technical research field in the search for new low-cost versatile materials for solar energy conversion and optoelectronics.[1−3] The current density−voltage (j−V) performance characteristic of a solar cell is the central property that provides the main parameters of steady-state behavior, namely, the photovoltage (V_{oc}), short-circuit current (j_{sc}), and fill factor (FF), which when combined establish the power conversion efficiency at the specified solar cell conditions. Measuring the j−V curve necessitates a dynamic measurement involving the sweeping of the voltage V at least from open circuit to short circuit, or vice versa, while recording the current density j, which should provide a stable response representing the long-term operation values of the solar cell under sunlight. Dynamic hysteresis of perovskite solar cells is the set of phenomena that make the current values fluctuate upon voltage cycling depending on details of measurement.

Since the advent of perovskite solar cells, dynamic hysteresis has been found to affect widely the supposedly steady-state performance.[4−6] The photocurrent displays diverse and sometimes apparently random behavior as a function of the starting voltage, the scan velocity $b = dV/dt$, and the delay time Δt between two consecutive voltage steps.[6,7] This behavior casts doubt on the validity of the performance values that are measured and reported, and it questions the efforts to improve the solar cell, requiring careful protocols to ensure a stabilized response.[8,9] Dynamic hysteresis has been found in several types of solar cells in the past, but it is especially challenging in the lead halide perovskite solar cell because it is a very large effect in typical slow measuring times, and the phenomenology is widely varied. According to an extended opinion, the dynamic hysteresis indicates the existence of physical phenomena occurring in the perovskite solar cell that need to be understood. Some authors have reported hysteresis-free devices,[10] but unfortunately, these are yet marginal in the field and do not represent most of the work that is currently being carried out in the area. There is no shortage of explanations for the frequently observed hysteresis using a wide set of different hypotheses, mainly involving traps, ion motion, band bending, boundary layers, grain boundaries, and other factors. Obviously, all these models capture to some extent the specific qualities of the hysteresis in current−voltage curves. What has not been achieved to date is a systematic and predictive model of how the different observed dynamic hysteresis effects depend on the previous conditioning and specific protocol of measurement. Furthermore, the model should have physical meaning consistent with observation obtained for different experimental techniques.

Received: January 8, 2017
Accepted: February 7, 2017
Published: February 7, 2017

DOI: 10.1021/acs.jpclett.7b00045
J. Phys. Chem. Lett. 2017, 8, 915−921

In this work, we will first describe the main trends of experimental observations reported to date, following which we will introduce a model based on the observation that the interface can be charged electronically that will quantitatively explain important characteristic features of phenomenology, consistent with dominant features previously observed by impedance spectroscopy and time transient methods. We will finish by showing experimental support that explains dynamic hysteresis in terms of large transient currents predicted by the surface polarization model and by calculating physical parameters by direct fitting of $j-V$ curves measured at different conditions.

Characteristic Features of Dynamic Hysteresis in Perovskite Solar Cells. We start the description of the features of dynamic hysteresis. In this Letter, forward (F) is the voltage around open circuit, and reverse (R) is the voltage beyond short circuit. For example, we can sweep the voltage in the direction FR or in the other direction, RF. However, a FR scan if we cycled continuously in both directions will be very different from the scan if we wait a little bit with the cell sitting at constant F bias beyond V_{oc} for a "preconditioning" or poling time. The value of the current will be characteristically larger, and the efficiency is amplified. To check the stability of the response, one usually cycles RF and backward FR, and the result of such a procedure is currently indispensable experimental evidence for reporting. However, making FR and RF in separate runs turns out to be very different than cycling the solar cell continuously. The sensitivity of dynamic hysteresis to the details of measurements has thus been broadly acknowledged. The work of Unger et al.[7] provided a sound recognition of these phenomena and the influence of the ionic conduction effects on the varying behaviors of the solar cells. Recent works have emphasized the role of contacts and ion migration effects in the occurrence of hysteresis and long-time stability.[11,12]

In the very large number of published results, we can distinguish a specific set of characteristic patterns that need to be explained by models of dynamic hysteresis. These patterns are shown schematically in Figure 1 and can be described as follows. Additional discussion, references, and experimental measurements are presented in the Supporting Information.

(a) Capacitive hysteresis. This behavior can be readily understood as an instantaneous capacitive current added on the steady-state diode curve.[4,10,13−16] Here, it is apparent that the nonsteady-state curves with the same voltage scan rate but opposite scan direction are symmetrically disposed with respect to the steady-state current, and additionally, the capacitive current increases linearly with scan rate.

(b) Starting from F to R, the current displays a maximum ("bump") and decreases to a stable photocurrent so that current close to V_{oc} is actually higher than short-circuit current. This phenomenon has been widely observed with a typical direct dependence on the time and/or value of poling in forward bias.[7,17−19] Different from case a, the RF scans have no symmetry with respect to the steady-state curve and are quite dependent on the time and/or value of reverse polarization.

(c) Apparent photocurrent enhancement in FR direction. When increasing the scan rate b, a plateau current is achieved (as in normal diode behavior) that increases significantly the final photocurrent with increasing scan rate.[7,18−20] Here, j_{sc} is modified while the low forward bias resistance and V_{oc} are unaltered. Unlike a and similarly to b, the RF curves are very sensitive to other experimental parameters, and diverse forms can be delivered.

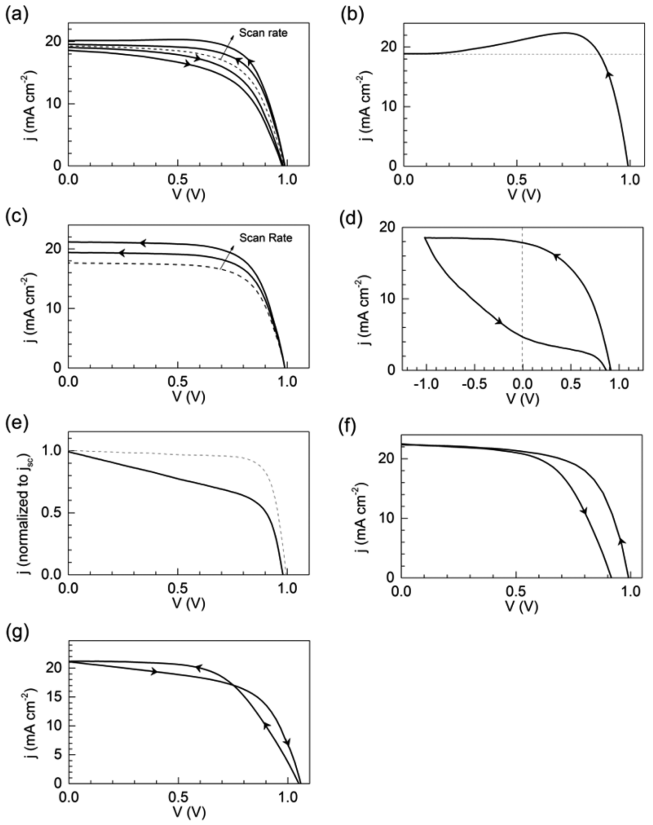

Figure 1. Characteristic patterns of hysteresis behavior in perovskite solar cells. The large arrows on the solid black lines indicate the scan sense. The black dashed lines show the steady-state curve (a, c). In panels b and d, the auxiliary dashed lines signal j_{sc} and zero applied bias respectively, while in panel e, it represents a typical diode curve.

(d) Strong decay of photocurrent in RF direction. This behavior has been reported[19−21] as a result of specific polarization routines. In a possibly related extreme case, the RF photocurrent achieves the opposite sign.[22,23]

(e) Remarkable ohmic-like behavior at low forward and reverse applied bias. The current increases in FR direction in an apparent shunt resistance effect; however, it is dependent on bias, scan rate and direction,[17−20] illumination,[7,24] and temperature.[17] This feature also modifies the j_{sc}.

(f) Apparent V_{oc} shift. The RF measurement delivers a V_{oc} that is lower than the one for the FR curve.[24−26] Here, the j_{sc} and the resistance at low forward bias are not modified. Subsequently, a mismatch between initial and final current after a loop may occur.[25]

(g) Crossing between curves at the same scan rate with opposite directions. Here, the RF curve exceeds the FR within some region between short circuit and open circuit,[10,24,25] unlike all previous patterns where the absolute current in RF direction is always lower than that in FR direction. Furthermore, the crossing can occur at low forward or reverse bias, meaning that a larger current is achieved for the RF scan in practically the whole first quadrant (larger FF).[27]

It should be also remarked that hysteretic effects practically disappear at room temperature when fullerene contacts are used instead of TiO_2 as electron-transport material. This indicates that ion migration is a necessary but not sufficient condition for interfacial accumulation to occur. The fact that fullerene-based perovskite solar cells do not exhibit significant capacitance in excess of the geometrical value corroborates the

DOI: 10.1021/acs.jpclett.7b00045
J. Phys. Chem. Lett. 2017, 8, 915−921

interface polarization origin of the hysteresis.[28] Several papers have explored specific features of the TiO_2/perovskite interface responsible for its charge accumulation ability. Ti−I bonds easily accommodate excess or defect ionic charge in a highly reversible way causing the capacitive currents.[29] Also, the morphology (disorder degree) at the interface has been related to hysteresis reduction, signaling that $CH_3NH_3PbI_3$ at the interface should be both homogeneous and crystalline.[12] With respect to the role of anodes (HTL/perovskite contacts), several recent papers have directly observed that charge accumulation at the TiO_2 interface is larger than that occurring at *spiro*-OMeTAD/perovskite interfaces. Weber and co-workers[30] have shown that the positive space-charge near the TiO_2 contact exceeds that at the HTL. We also observed by comparing symmetrical devices of structure TiO_2/perovskite/TiO_2 and *spiro*-OMeTAD/perovskite/*spiro*-OMeTAD, that it is precisely the TiO_2/perovskite interface that is able to reversibly accumulate charge producing capacitive currents while *spiro*-OMeTAD contacts do not.[31]

Physical Effects Leading to Dynamic Hysteresis in Perovskite Solar Cells. In the literature, there are two main models based on detailed simulation of the transport−recombination approach. The model of Snaith and co-workers[32] combines ionic drift and surface trapping to explain the pattern in Figure 1d, but this model does not systematically implement dynamic scans. On the other hand, Walker and co-workers[21] describe the solar cell as a macrocapacitor where ions can be accumulated at the interface. This model reproduces by this feature the capacitive properties observed in experiments and also describes well the large asymmetry in Figure 1d; however, the electronic features are simplified and the $j-V$ curve is described in terms of charge collection controlled by the electric field. Therefore, the model cannot describe the wide phenomenology mentioned before.

Our approach in this Letter is to design a simple model that captures the physical core of the dynamic hysteresis without the burden of massive computational cost. In early work, a persistent voltage was observed in photovoltage decays spanning such a long time scale that it was concluded that it cannot be due to electronic recombination alone.[33,34] Many authors have attributed the slow modification of the cell response to the ion redistribution,[35−37] but the central question is how the ionic effect influences the electronic features that are finally measured in $j-V$ performance. One natural possibility is to relate the ionic redistribution to the modification of charge collection efficiency by the changes of internal electric field in the solar cell.[20,21,36] However, the lead halide perovskite solar cell has extremely long diffusion length;[38,39] thus, the electric field should be a minor factor in the $j-V$ curve, unless in extreme situations. Such types of situation may be produced if the perovskite solar cell is polarized for a substantial period of time at reverse bias, in which case a drift of ions can heavily modify the condition of operation by establishing a pseudo built-in voltage that decreases the charge collection efficiency, as recognized by Tress et al.[20] and Walker and co-workers.[21] In fact, Snaith and co-workers[32] have nicely shown that the feature of Figure 1d becomes more pronounced when the poling voltage becomes progressively more reverse. Under exaggerated pretreatment, the contacts can be severely modified so that the solar cell can be forced to produce negative values of the photocurrent.[23] However, we show in Figure SI1d that one can also observe the characteristic features of dynamic hysteresis in the dark, which therefore cannot be primarily due to changes of charge collection properties. It has also been shown[14] that if a scan goes in the RF direction at successive voltage steps without pretreatment at R, and then FR, only the instantaneous capacitive behavior with a symmetric current around the steady-state value is observed, as in Figure 1a. Thus, the spurious reverse prepolarization effects can be avoided. Therefore, we leave these phenomena arising from sustained forcing of the cell at R bias out of the scope of our model in which we will analyze the FR scan predominantly.

Evidence from Capacitance Results for Surface Polarization. Our model is based on the observation that in F polarization, the interface can be charged electronically (with electrons and holes at either side of the interface), which creates a significant transient current that causes a strong hysteresis effect in a FR scan measurement. This picture is consistent with several physical observations on the operation of hybrid perovskite solar cells.[19,26,30,40−42] As we know from plenty of evidence, the interfaces can be affected by strong electronic charging assisted by the presence of mobile ions.[15,37,40,41] The meaning of capacitance versus frequency has been well-understood.[43,44] The low-frequency large capacitance in the dark is associated with the ionic polarization at the perovskite interface with the contact, whereas the higher-frequency plateau is a dielectric polarization in the bulk of the perovskite.[15,45] An interpretation of the huge capacitance observed under illumination was suggested by Zarazua et al. in terms of accumulation of majority carriers at the interface.[40] They provided a picture of an electrostatic component to the photovoltage, produced by upward band bending at the electron contact. Gottesmann et al. showed that the electrostatic photovoltage can explain long time transients in open-circuit voltage decay.[41] This observation does not rule out the presence of interfacial electronic states at the contact that may produce slow kinetic effects. However, as it is shown later, the charge stored is so large that traps cannot explain this effect; therefore, trapping of carriers is not a primary consideration in our model.

However, why is the kinetics of the large capacitance very slow? This question was analyzed with a study of photovoltage decay as a function of illumination preconditioning.[41] By combining the analysis of decays and detailed simulation of the interface, it was found that accumulation of cations at the interface assists the formation of the electronic accumulation. Previously, the decay of external voltage was described by the relaxation of voltage.[34] Pintillie and co-workers[19] have provided a model description of the dynamic hysteresis under cycling in terms of internal depolarization, but their model is for a dielectric relaxation. Weber and co-workers identified in situ the distribution of space charge across the absorber layer, situated at the contact interfaces.[30] A correlation between interfacial capacitance and the amount of hysteresis was realized,[27,46] and especially the TiO_2 electron contact displays an enormous capacitance combined with a large hysteresis effect.

According to the previous observations, the interface changes dramatically with the voltage, producing a huge accumulation of charge, with the kinetics controlled by ion diffusion. Interface recombination is a major impediment to charge collection. The diffusion of ions and its influence on the global electrical field appear to be of secondary interest, rather it is the accumulation of ions at the interface and their rate of arrival and departure from there that are the central effects governing the operational properties of the cell.

DOI: 10.1021/acs.jpclett.7b00045
J. Phys. Chem. Lett. 2017, 8, 915−921

Surface Polarization Model of Dynamic Hysteresis. The description of $j-V$ curve measurement results in Figure 1 requires a model for the current obtained under illumination when we sweep the voltage at rate b. We now describe such a model based on the diagrams of Figure 2. The main assumption

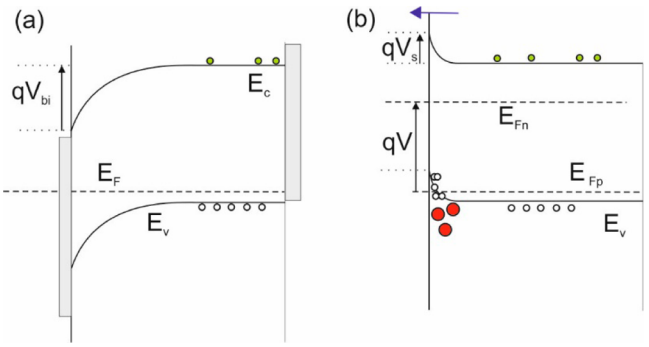

Figure 2. Schematic representation of the energy diagram of a perovskite solar cell with electron-selective contact at the left and hole-selective contact at the right side. (a) Equilibrium in the dark. (b) Open-circuit under illumination. E_c and E_v, edges of conduction and valence band, respectively; E_F, Fermi level; E_{Fn} and E_{Fp}, quasi-Fermi level of electrons and holes, respectively; V, external voltage of the contacts; V_{bi}, constant built-in voltage; V_s, variable surface polarization voltage. Indicated in panel b are the accumulation of holes and cations and the tunnelling of electrons across the surface barrier. Note that electrons at the contact side of the interface that contribute to charge compensation are not shown.

adopted here is a distinction of the external voltage, V, and the surface polarization voltage, V_s. The former corresponds to the voltage at the contacts which can be changed instantaneously, while V_s is an internal voltage by upward bending at the surface that responds by internal kinetics and determines the excess charge density of holes at the interface.[40,41] In a first approximation, the surface charge is

$$Q_s = qp_s = Q_{s0}\exp(qV_s/\gamma k_B T) \tag{1}$$

in terms of surface hole density p_s, the elementary electrical charge q, the thermal energy $k_B T$, and a general exponent γ that in the ideal case takes the value 2. The accumulation capacitance is

$$C_{acc} = \frac{dQ_s}{dV_s} = \frac{qQ_{s0}}{\gamma k_B T}\exp(qV_s/\gamma k_B T) \tag{2}$$

The surface charge parameter can be estimated from the following expression,[40] where p_0 is the equilibrium hole density

$$Q_{s0} = \sqrt{2}\, qp_0 L_D \tag{3}$$

and L_D is the Debye length

$$L_D = \sqrt{\varepsilon\varepsilon_0 k_B T/q^2 p_0} \tag{4}$$

At steady-state conditions at a given voltage V, the surface polarization depends on the built-in potential V_{bi} as follows:

$$V_s = V - V_{bi} \tag{5}$$

However, as described before, the interfacial charge distribution is strongly determined by the presence of ions;[41] therefore, V_s cannot instantaneously follow the external voltage. Considering that the internal voltage V_s strives for the equilibrium condition indicated in eq 5, we propose a kinetic condition of the type

$$\frac{dV_s}{dt} = -\frac{V_s - (V - V_{bi})}{\tau_{kin}} \tag{6}$$

where the relaxation kinetic constant, τ_{kin}, should be determined by the rapidity of ion displacement at the given illumination and temperature.[17,19,34,47] Note that eq 6 is a central assumption that combines the dynamics and distribution of surface charge (ionic and electronic). A more elaborate model could be based on detailed charge compensation at the surface given by the expression

$$Q_s + qc_c = qn_{etl} \tag{7}$$

where c_c is the surface density of cations and n_{etl} is the density of electrons in the outer electron-transport layer.

Recombination current at the surface[42] depends on both electron and hole concentration

$$j_{rec} = k_{rec} n Q_s \tag{8}$$

with a recombination rate constant k_{rec}. The bulk electron density is $n = n_0\exp(qV/\beta k_B T)$, where $\beta = 1$ is the ideal parameter value. Hence, the recombination current in transient conditions is

$$j_{rec} = j_{rec0}\exp(qV_{bi}/\gamma k_B T)\exp[q(V_s/\gamma + V/\beta)/k_B T] \tag{9}$$

where the recombination parameter is

$$j_{rec0} = k_{rec} Q_{s0} n_0 \exp(-qV_{bi}/\gamma k_B T) \tag{10}$$

The extracted current is composed of the photocurrent j_{ph} minus the transient recombination current. To these terms, we add the current of extracted excess electrons from the contact layer, which at strong F bias is $qn_{etl} \approx Q_s$. Hence

$$j = j_{ph} - j_{rec0}\exp(qV_{bi}/\gamma k_B T)\exp[q(V_s/\gamma + V/\beta)/k_B T] + \frac{dQ_s}{dt} \tag{11}$$

Modifying the last term, we obtain

$$j = j_{ph} - j_{rec0}\exp[q(V_s/\gamma + V/\beta + V_{bi}/\gamma)/k_B T] + C_{acc}\frac{dV_s}{dt} \tag{12}$$

The steady-state current is obtained by imposing the equilibrium value of surface voltage determined by the external potential, eq 5. Including the constant dark current in reverse, we obtain the diode equation

$$j = j_{ph} + j_{rec0}[\exp(qV/mk_B T) - 1] \tag{13}$$

where

$$m = \frac{\beta\gamma}{\beta + \gamma} \tag{14}$$

The model is complete and allows the calculation of the results of a number of techniques. In this Letter, we treat only the usual voltage ramp in the direction FR, which consists of the time dependence

$$V = V_{in} + bt \tag{15}$$

where V_{in} is the initial voltage and the scan rate b is negative. We assume that the system starts at steady-state condition at V_{in}. We also define the initial surface voltage

$$V_{s0} = V_{in} - V_{bi} \tag{16}$$

DOI: 10.1021/acs.jpclett.7b00045
J. Phys. Chem. Lett. 2017, 8, 915−921

The analytical solution to these conditions is described in the Supporting Information. A summary of the pertinent features of the $j-V$ curves simulated from our model is shown in Figure 3,

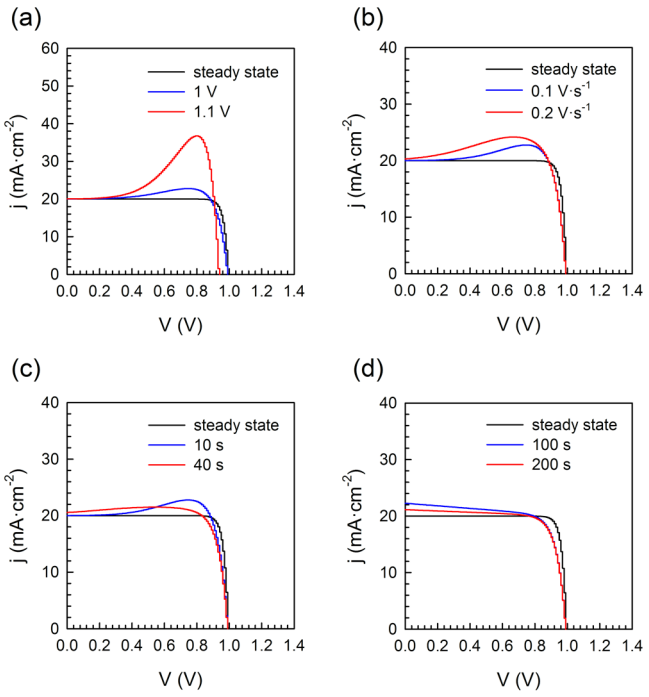

Figure 3. Simulated FR $j-V$ curves for different (a) initial voltages, V_{in}; (b) scan rates; (c) small τ_{kin}; and (d) large τ_{kin} for $b = 100$ kV·s^{-1}. The parameters for the curves were $Q_{s0} = 4.4 \times 10^{-8}$ C·cm^{-2}, $b = 100$ mV·s^{-1}, $V_{bi} = 350$ mV, $\beta = 2$, $\gamma = 2$, $j_{ph} = 20$ mA·cm^{-2}, $j_{rec0} = 4.8 \times 10^{-16}$ mA·cm^{-2}, $\tau_{kin} = 10$ s for panels a and b.

with a simulated RF scan also shown in Figure SI2a. The surface polarization decay yields a "bump" in the current whose magnitude increases with increasing V_{in} and also with increasing scan rate, as shown in Figure 3a,b. This bump and its evolution is well-documented in the literature and has already been depicted in Figure 1b. This bump eventually decays down to the photocurrent value depending on the kinetic relaxation time, τ_{kin}. If the kinetic delay time is large enough compared to the scan rate, the obtained short-circuit current value is higher than the maximum photocurrent value, as shown in Figure 3c. For very large scan rates and large τ_{kin} values, we obtain the apparent photocurrent enhancement with the plateau as in a normal diode as described earlier in Figure 3d. The slope of this plateau depends inversely on τ_{kin}; see the Supporting Information for the mathematical expression. We have also simulated the effect of a reduced accumulation layer at the contacts on the performance of the cell (Figure SI2b).

Model Description of Experimental Results of Dynamic Hysteresis. As our model successfully reproduced several of the typical behaviors of FR dynamic hysteresis, we then proceeded to fit some experimental FR $j-V$ curves for $CH_3NH_3PbI_3$ perovskite for different V_{in} to obtain relevant parameters of the model. We have measured the $j-V$ curves at different forward polarization values which provide increasing values of the bump in FR measurement, as shown in Figure 4a. To describe such curves is a challenge because traps at the electron contact should be saturated at large forward bias so that the observed changes cannot be explained only by detrapping effects. On the other hand, an accumulation

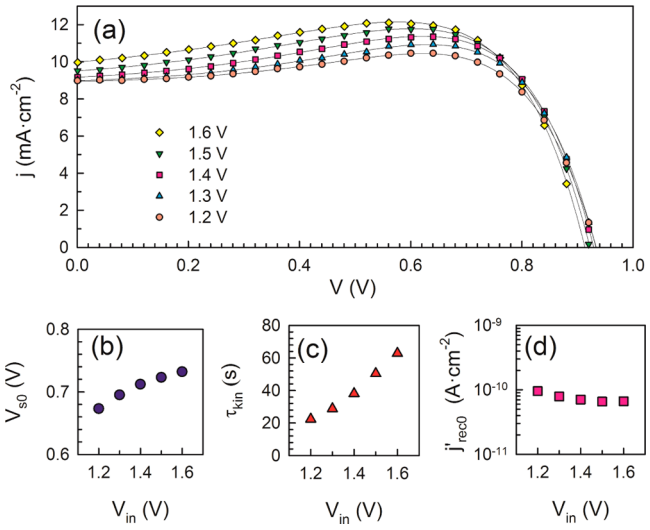

Figure 4. Hysteresis in FR scans of $TiO_2/CH_3NH_3PbI_3$/spiro-OMeTAD solar cell and the fittings of the surface polarization model. (a) Experimental FR $j-V$ curves measured at $b = 100$ mV/s (symbols) and corresponding fitted curves (lines) for different initial applied voltage, V_{in}, as indicated. Parameters (b) V_{s0}, (c) τ_{kin}, and (d) $j_{rec0} \exp(qV_{bi}/2k_BT)$ obtained from least-squares fitting.

capacitance does not have any limitation for additional charging at increasing forward bias as indicated in eq 1, and it explains very well the growing current by the release of the accumulated charge.

Here we employed a least-squares fitting method consisting of a maximum of seven free parameters, namely, Q_{s0}, V_{s0}, τ_{kin}, $j'_{rec0} = j_{rec0} \exp(qV_{bi}/2k_BT)$, j_{ph}, β, and γ. The values of Q_{s0} and $\gamma = 2$ were estimated based on the accumulation capacitance of eqs 2 and 3. For a doping density of 10^{17} cm^{-3} and relative dielectric constant $\varepsilon = 26$, we obtained $Q_{s0} = 4.4 \times 10^{-8}$ C·cm^{-2}. Subsequent fittings of the experimental data yielded an average value for β of 6, which was used to fix this parameter in the model. Note that this means a diode ideality factor value of $m = 1.5$, expressed in eq 14. The final fitting lines obtained with fixed Q_{s0}, β, and γ parameters and their evolution with respect to V_{in} are shown in Figure 4, and they provide excellent agreement with the data.

We observe in Figure 4b that the initial surface voltage V_{s0} increases sluggishly with the applied voltage as $V_{s0} \approx V_{in}/2$. Given that V_{bi} in eq 16 is a constant, this discrepancy could be related to the fact that the accumulation at the interface depends strongly on several factors such as poling time, the kinetic relaxation time of the ions, and the interfacial properties of the contact, leading to deviations from our simplified model. A more complete model using detailed simulation of the interface incorporating eq 7 could account for these variations; nevertheless, we consider that our simplified model gives an excellent physical description of the charge accumulation and its release, explaining the dynamic hysteresis in FR scan. The suitability of our model for dynamic hysteresis is further confirmed by the fact that the accumulation charge calculated from eq 1 and that obtained by integrating the transient part of the $j-V$ curves closely match; the corresponding charge values are given in Figure SI3. The kinetic relaxation time itself evolves linearly with V_{in}, which is expected, as the large upward band bending of the accumulation layer, which increases with V_{in}, slows down the flow of cations away from the interface. These obtained parameters can therefore serve as a good reference

DOI: 10.1021/acs.jpclett.7b00045
J. Phys. Chem. Lett. 2017, 8, 915−921

point for understanding the nature of the accumulation at the interface and recombination in perovskite solar cells, while providing useful information about internal parameters of the cell in a rather simplistic manner.

In conclusion, we have developed a dynamic hysteresis model based on the charging of the contact interface by the formation of an accumulation layer of holes and ions compensated by electrons at the contact. This surface voltage strives for the equilibrium condition based on a kinetic relaxation time of displacement of the ions, leading to a discharge current upon cycling the voltage. By including surface recombination, we reproduce many of the observed cases of experimental hysteresis in perovskites depending on experimental parameters such as the poling voltage and the scan rate. The model provides a quantitative explanation of different typical hysteretic features that occur in measurements from forward to reverse voltage scans. Our results highlight that hysteresis can be explained by ionic movement and electrode polarization exclusively without the effect of trap-assisted recombination. The detailed analytical equations establish for the first time the possibility of systematically investigating quantitatively the effect of previous conditions applied to the solar cell. Furthermore, the model is consistent with other methods such as impedance spectroscopy, open-circuit voltage decays, and Kelvin probe scan methods, which opens the opportunity to investigate by different independent methodologies the peculiar kinetic phenomena widely observed in perovskite solar cells.

■ ASSOCIATED CONTENT

Supporting Information

The Supporting Information is available free of charge on the ACS Publications website at DOI: 10.1021/acs.jpclett.7b00045.

Preparation methods, features of current−voltage curves, analytical solutions of $j-V$ curves, and acccumulated charge at the interface (PDF)

■ AUTHOR INFORMATION

Corresponding Author

*E-mail: bisquert@uji.es.

ORCID

Sandheep Ravishankar: 0000-0002-8118-0159

Francisco Fabregat-Santiago: 0000-0002-7503-1245

Germà Garcia-Belmonte: 0000-0002-0172-6175

Juan Bisquert: 0000-0003-4987-4887

Notes

The authors declare no competing financial interest.

■ ACKNOWLEDGMENTS

We acknowledge funding from MINECO of Spain under Project MAT2016-76892-C3-1-R and Generalitat Valenciana Project PROMETEOII/2014/020. S.R. and O.A. acknowledge Generalitat Valenciana for Grants GRISOLIA/2014/034 and GRISOLIA/2014/035, respectively.

■ REFERENCES

(1) Kojima, A.; Teshima, K.; Shirai, Y.; Miyasaka, T. Organometal Halide Perovskites as Visible-Light Sensitizers for Photovoltaic Cells. *J. Am. Chem. Soc.* **2009**, *131*, 6050−6051.

(2) Park, N.-G.; Grätzel, M.; Miyasaka, T. *Organic-Inorganic Halide Perovskite Photovoltaics: From Fundamentals to Device Architectures*, 1st ed.; Springer: Cham, Switzerland, 2016; p VIII.

(3) Lee, M. M.; Teuscher, J.; Miyasaka, T.; Murakami, T. N.; Snaith, H. J. Efficient Hybrid Solar Cells Based on Meso-Superstructured Organometal Halide Perovskites. *Science* **2012**, *338*, 643−647.

(4) Sanchez, R. S.; Gonzalez-Pedro, V.; Lee, J.-W.; Park, N.-G.; Kang, Y. S.; Mora-Sero, I.; Bisquert, J. Slow Dynamic Processes in Lead Halide Perovskite Solar Cells. Characteristic Times and Hysteresis. *J. Phys. Chem. Lett.* **2014**, *5*, 2357−2363.

(5) Snaith, H. J.; Abate, A.; Ball, J. M.; Eperon, G. E.; Leijtens, T.; Noel, N. K.; Stranks, S. D.; Wang, J. T.-W.; Wojciechowski, K.; Zhang, W. Anomalous Hysteresis in Perovskite Solar Cells. *J. Phys. Chem. Lett.* **2014**, *5*, 1511−1515.

(6) Kim, H.-S.; Park, N.-G. Parameters Affecting I−V Hysteresis of $CH_3NH_3PbI_3$ Perovskite Solar Cells: Effects of Perovskite Crystal Size and Mesoporous TiO_2 Layer. *J. Phys. Chem. Lett.* **2014**, *5*, 2927−2934.

(7) Unger, E. L.; Hoke, E. T.; Bailie, C. D.; Nguyen, W. H.; Bowring, A. R.; Heumuller, T.; Christoforo, M. G.; McGehee, M. D. Hysteresis and Transient Behavior in Current-Voltage Measurements of Hybrid-Perovskite Absorber Solar Cells. *Energy Environ. Sci.* **2014**, *7*, 3690−3698.

(8) Christians, J. A.; Manser, J. S.; Kamat, P. V. Best Practices in Perovskite Solar Cell Efficiency Measurements. Avoiding the Error of Making Bad Cells Look Good. *J. Phys. Chem. Lett.* **2015**, *6*, 852−857.

(9) Zimmermann, E.; Wong, K. K.; Müller, M.; Hu, H.; Ehrenreich, P.; Kohlstädt, M.; Würfel, U.; Mastroianni, S.; Mathiazhagan, G.; Hinsch, A.; et al. Characterization of Perovskite Solar Cells: Towards a Reliable Measurement Protocol. *APL Mater.* **2016**, *4*, 091901.

(10) Almora, O.; Aranda, C.; Zarazua, I.; Guerrero, A.; Garcia-Belmonte, G. Noncapacitive Hysteresis in Perovskite Solar Cells at Room Temperature. *ACS Energy Lett.* **2016**, *1*, 209−215.

(11) Domanski, K.; Roose, B.; Matsui, T.; Saliba, M.; Turren-Cruz, S.-H.; Correa-Baena, J.-P.; Carmona, C. R.; Richardson, G.; Foster, J. M.; De Angelis, F.; et al. Migration of Cations Induces Reversible Performance Losses over Day/Night Cycling in Perovskite Solar Cells. *Energy Environ. Sci.* **2017**, DOI: 10.1039/C6EE03352K.

(12) Patel, J. B.; Wong-Leung, J.; Van Reenen, S.; Sakai, N.; Wang, J. T. W.; Parrott, E. S.; Liu, M.; Snaith, H. J.; Herz, L. M.; Johnston, M. B. Influence of Interface Morphology on Hysteresis in Vapor-Deposited Perovskite Solar Cells. *Adv. Electron. Mater.* **2016**, 1600470.

(13) Chen, B.; Yang, M.; Zheng, X.; Wu, C.; Li, W.; Yan, Y.; Bisquert, J.; Garcia-Belmonte, G.; Zhu, K.; Priya, S. Impact of Capacitive Effect and Ion Migration on the Hysteretic Behavior of Perovskite Solar Cells. *J. Phys. Chem. Lett.* **2015**, *6*, 4693−4700.

(14) Ono, L. K.; Raga, S. R.; Remeika, M.; Winchester, A. J.; Gabe, A.; Qi, Y. Pinhole-Free Hole Transport Layers Significantly Improve the Stability of $MAPbI_3$-based Perovskite Solar Cells under Operating Conditions. *J. Mater. Chem. A* **2015**, *3*, 15451−15456.

(15) Almora, O.; Zarazua, I.; Mas-Marza, E.; Mora-Sero, I.; Bisquert, J.; Garcia-Belmonte, G. Capacitive Dark Currents, Hysteresis, and Electrode Polarization in Lead Halide Perovskite Solar Cells. *J. Phys. Chem. Lett.* **2015**, *6*, 1645−1652.

(16) Valles-Pelarda, M.; Hames, B. C.; García-Benito, I.; Almora, O.; Molina-Ontoria, A.; Sánchez, R. S.; Garcia-Belmonte, G.; Martín, N.; Mora-Sero, I. Analysis of the Hysteresis Behavior of Perovskite Solar Cells with Interfacial Fullerene Self-Assembled Monolayers. *J. Phys. Chem. Lett.* **2016**, *7*, 4622−4628.

(17) Ono, L. K.; Raga, S. R.; Wang, S.; Kato, Y.; Qi, Y. Temperature-Dependent Hysteresis Effects in Perovskite-Based Solar Cells. *J. Mater. Chem. A* **2015**, *3*, 9074−9080.

(18) Correa-Baena, J. P.; Steier, L.; Tress, W.; Saliba, M.; Neutzner, S.; Matsui, T.; Giordano, F.; Jacobsson, T. J.; Srimath Kandada, A. R.; Zakeeruddin, S. M.; et al. Highly Efficient Planar Perovskite Solar Cells through Band Alignment Engineering. *Energy Environ. Sci.* **2015**, *8*, 2928−2934.

(19) Nemnes, G. A.; Besleaga, C.; Tomulescu, A. G.; Pintilie, I.; Pintilie, L.; Torfason, K.; Manolescu, A. Dynamic Electrical Behavior of Halide Perovskite Based Solar Cells. *Sol. Energy Mater. Sol. Cells* **2017**, *159*, 197−203.

(20) Tress, W.; Marinova, N.; Moehl, T.; Zakeeruddin, S. M.; Nazeeruddin, M. K.; Gratzel, M. Understanding the Rate-Dependent J-

V Hysteresis, Slow Time Component, and Aging in $CH_3NH_3PbI_3$ Perovskite Solar Cells: The Role of a Compensated Electric Field. *Energy Environ. Sci.* **2015**, *8*, 995−1004.
(21) Richardson, G.; O'Kane, S. E. J.; Niemann, R. G.; Peltola, T. A.; Foster, J. M.; Cameron, P. J.; Walker, A. B. Can Slow-Moving Ions Explain Hysteresis in the Current-Voltage Curves of Perovskite Solar Cells? *Energy Environ. Sci.* **2016**, *9*, 1476−1485.
(22) Park, N.-G. Perovskite Solar Cells: Switchable Photovoltaics. *Nat. Mater.* **2015**, *14*, 140−141.
(23) Xiao, Z.; Yuan, Y.; Shao, Y.; Wang, Q.; Dong, Q.; Bi, C.; Sharma, P.; Gruverman, A.; Huang, J. Giant Switchable Photovoltaic Effect in Organometal Trihalide Perovskite Devices. *Nat. Mater.* **2015**, *14*, 193−198.
(24) Chen, B.; Yang, M.; Priya, S.; Zhu, K. Origin of J−V Hysteresis in Perovskite Solar Cells. *J. Phys. Chem. Lett.* **2016**, *7*, 905−917.
(25) Giorgi, G.; Yamashita, K. Zero-Dipole Molecular Organic Cations in Mixed Organic−Inorganic Halide Perovskites: Possible Chemical Solution for the Reported Anomalous Hysteresis in the Current−Voltage Curve Measurements. *Nanotechnology* **2015**, *26*, 442001.
(26) Contreras, L.; Idigoras, J.; Todinova, A.; Salado, M.; Kazim, S.; Ahmad, S.; Anta, J. A. Specific Cation Interactions as the Cause of Slow Dynamics and Hysteresis in Dye and Perovskite Solar Cells: a Small-Perturbation Study. *Phys. Chem. Chem. Phys.* **2016**, *18*, 31033−31042.
(27) Sepalage, G. A.; Meyer, S.; Pascoe, A.; Scully, A. D.; Huang, F.; Bach, U.; Cheng, Y.-B.; Spiccia, L. Copper(I) Iodide as Hole-Conductor in Planar Perovskite Solar Cells: Probing the Origin of J−V Hysteresis. *Adv. Funct. Mater.* **2015**, *25*, 5650−5661.
(28) Garcia-Belmonte, G.; Bisquert, J. Distinction between Capacitive and Noncapacitive Hysteretic Currents in Operation and Degradation of Perovskite Solar Cells. *ACS Energy Lett.* **2016**, *1*, 683−688.
(29) Roiati, V.; Mosconi, E.; Listorti, A.; Colella, S.; Gigli, G.; De Angelis, F. Stark Effect in Perovskite/TiO_2 Solar Cells: Evidence of Local Interfacial Order. *Nano Lett.* **2014**, *14*, 2168−2174.
(30) Bergmann, V. W.; Guo, Y.; Tanaka, H.; Hermes, I. M.; Li, D.; Klasen, A.; Bretschneider, S. A.; Nakamura, E.; Berger, R.; Weber, S. A. L. Local Time-Dependent Charging in a Perovskite Solar Cell. *ACS Appl. Mater. Interfaces* **2016**, *8*, 19402−19409.
(31) Carrillo, J.; Guerrero, A.; Rahimnejad, S.; Almora, O.; Zarazua, I.; Mas-Marza, E.; Bisquert, J.; Garcia-Belmonte, G. Ionic Reactivity at Contacts and Aging of Methylammonium Lead Triiodide Perovskite Solar Cells. *Adv. Energy Mater.* **2016**, *6*, 1502246.
(32) van Reenen, S.; Kemerink, M.; Snaith, H. J. Modeling Anomalous Hysteresis in Perovskite Solar Cells. *J. Phys. Chem. Lett.* **2015**, *6*, 3808−3814.
(33) Baumann, A.; Tvingstedt, K.; Heiber, M. C.; Väth, S.; Momblona, C.; Bolink, H. J.; Dyakonov, V. Persistent Photovoltage in Methylammonium Lead Iodide Perovskite Solar Cells. *APL Mater.* **2014**, *2*, 081501.
(34) Bertoluzzi, L.; Sanchez, R. S.; Liu, L.; Lee, J.-W.; Mas-Marza, E.; Han, H.; Park, N.-G.; Mora-Sero, I.; Bisquert, J. Cooperative Kinetics of Depolarization in $CH_3NH_3PbI_3$ Perovskite Solar Cells. *Energy Environ. Sci.* **2015**, *8*, 910−915.
(35) Azpiroz, J. M.; Mosconi, E.; Bisquert, J.; De Angelis, F. Defects Migration in Methylammonium Lead Iodide and their Role in Perovskite Solar Cells Operation. *Energy Environ. Sci.* **2015**, *8*, 2118−2127.
(36) Eames, C.; Frost, J. M.; Barnes, P. R. F.; O'Regan, B. C.; Walsh, A.; Islam, M. S. Ionic Transport in Hybrid Lead Iodide Perovskite Solar Cells. *Nat. Commun.* **2015**, *6*, 7497.
(37) Almora, O.; Guerrero, A.; Garcia-Belmonte, G. Ionic Charging by Local Imbalance at Interfaces in Hybrid Lead Halide Perovskites. *Appl. Phys. Lett.* **2016**, *108*, 043903.
(38) Stranks, S. D.; Eperon, G. E.; Grancini, G.; Menelaou, C.; Alcocer, M. J. P.; Leijtens, T.; Herz, L. M.; Petrozza, A.; Snaith, H. J. Electron-Hole Diffusion Lengths Exceeding 1 Micrometer in an Organometal Trihalide Perovskite Absorber. *Science* **2013**, *342*, 341−344.
(39) Xing, G.; Mathews, N.; Sun, S.; Lim, S. S.; Lam, Y. M.; Grätzel, M.; Mhaisalkar, S.; Sum, T. C. Long-Range Balanced Electron- and Hole-Transport Lengths in Organic-Inorganic $CH_3NH_3PbI_3$. *Science* **2013**, *342*, 344−347.
(40) Zarazua, I.; Bisquert, J.; Garcia-Belmonte, G. Light-Induced Space-Charge Accumulation Zone as Photovoltaic Mechanism in Perovskite Solar Cells. *J. Phys. Chem. Lett.* **2016**, *7*, 525−528.
(41) Gottesman, R.; Lopez-Varo, P.; Gouda, L.; Jimenez-Tejada, J. A.; Hu, J.; Tirosh, S.; Zaban, A.; Bisquert, J. Dynamic Phenomena at Perovskite/Electron-Selective Contact Interface as Interpreted from Photovoltage Decays. *Chem.* **2016**, *1*, 776−789.
(42) Guerrero, A.; Garcia-Belmonte, G.; Mora-Sero, I.; Bisquert, J.; Kang, Y. S.; Jacobsson, T. J.; Correa-Baena, J.-P.; Hagfeldt, A. Properties of Contact and Bulk Impedances in Hybrid Lead Halide Perovskite Solar Cells Including Inductive Loop Elements. *J. Phys. Chem. C* **2016**, *120*, 8023−8032.
(43) Bisquert, J.; Garcia-Belmonte, G.; Mora-Sero, I. Characterization of Capacitance, Transport and Recombination Parameters in Hybrid Perovskite and Organic Solar Cells. In *Unconventional Thin Film Photovoltaics*; Como, E. D., Angelis, F. D., Snaith, H., Walker, A., Eds.; The Royal Society of Chemistry: London, 2016.
(44) Bisquert, J.; Garcia-Belmonte, G.; Guerrero, A. Impedance Characteristics of Hybrid Organometal Halide Perovskite Solar Cells. In *Organic-Inorganic Halide Perovskite Photovoltaics: From Fundamentals to Device Architectures*; Park, N.-G., Grätzel, M., Miyasaka, T., Eds.; Springer: Cham, Switzerland, 2016.
(45) Almora, O.; Aranda, C.; Mas-Marzá, E.; Garcia-Belmonte, G. On Mott-Schottky Analysis Interpretation of Capacitance Measurements in Organometal Perovskite Solar Cells. *Appl. Phys. Lett.* **2016**, *109*, 173903.
(46) Kim, H.-S.; Jang, I.-H.; Ahn, N.; Choi, M.; Guerrero, A.; Bisquert, J.; Park, N.-G. Control of I−V Hysteresis in $CH_3NH_3PbI_3$ Perovskite Solar Cell. *J. Phys. Chem. Lett.* **2015**, *6*, 4633−4639.
(47) Bryant, D.; Wheeler, S.; O'Regan, B. C.; Watson, T.; Barnes, P. R. F.; Worsley, D.; Durrant, J. Observable Hysteresis at Low Temperature in "Hysteresis Free" Organic−Inorganic Lead Halide Perovskite Solar Cells. *J. Phys. Chem. Lett.* **2015**, *6*, 3190−3194.

DOI: 10.1021/acs.jpclett.7b00045
J. Phys. Chem. Lett. 2017, 8, 915−921